Control of excitable pulses in an injection-locked semiconductor laser

M. Turconi, B. Garbin, M. Feyereisen, M. Giudici, and S. Barland
Université de Nice, CNRS UMR 7335, Institut Non Linéaire de Nice, 1361 route des lucioles 06560 Valbonne, France

In spite of numerous theoretical and experimental reports of excitability in lasers with injected signal based on the locking-unlocking transition, the response of the system to controlled external perturbations (which is at the basis of the definition of excitable systems) has not been experimentally studied yet. In the following, we analyze the response of an injection-locked semiconductor laser to different external perturbations. We demonstrate the existence of a perturbation threshold beyond which the response of the system is independent of the strength of the stimulation and, thus, demonstrate its excitable character. We show that optically perturbing such an excitable system via the control of the phase of the injection beam can be useful for optical pulse generation.

Excitable systems (defined by their threshold-like, well-defined response to external perturbations) have been observed in a number of contexts, the paradigmatic example being found in physiology with the seminal measurements of current-voltage relations in the membrane of the giant axon of loligo [1]. Progress in the theoretical understanding of the dynamical mechanisms that make a system "excitable," which has been inspired by biology [2–4] and chemistry (see, for example, Ref. [5]), has naturally established the ubiquity of the feature. For example, in the context of optics, the excitable response of systems to external stimuli has been observed experimentally in several settings, including lasers with saturable absorber [6–8], semiconductor lasers with optical feedback [9], or optical injection [10], silicon microrings [11], and photonic crystals [12,13].

One specific mechanism expected to bring a laser system to an excitable state is the vicinity in parameter space of a saddle node on a circle bifurcation [14]. This situation is expected to arise when a laser with coherent optical injection is locked to the external forcing and brought close to the unlocking transition. In this parameter regime, a minimal (and, of course, forcibly incomplete) description of the system is given by the so-called Adler equation [15], which generically describes the behavior of a damped and forced oscillator. This exact situation has been analyzed experimentally with different semiconductor laser systems and large excursions in phase space have been interpreted as noise-triggered excitable pulses [16–18]. However, even though it is the *defining* property of an excitable system, the actual response of such a system to controlled external perturbations has not been analyzed yet.

In the experiment described below, we place an injection-locked semiconductor laser close to the unlocking transition and we observe its response to different kinds of external perturbations. This analysis is important from at least two points of view: first, it constitutes the first actual demonstration of the control of excitable pulses based on the locking-unlocking transition in a laser with injected signal; second, it actually opens the way to making use of such an excitable system when put in interaction with the outside world. In fact, any application of excitability (for instance to event detection [19] or image processing [20] or even more ambitious information processing schemes possibly involving coupled systems) will require proper knowledge of how to input

information into the system, i.e., of how to trigger an excitable response of the system.

The experimental setup we use is based on a vertical cavity surface emitting laser (VCSEL) under optical injection (Fig. 1). The VCSEL (ULM980-03-TN-S46) emits at 980 nm on the fundamental transverse mode from threshold (0.2 mA) up to more than 2 mA. We have also checked that it emits on a single linear polarization mode up to 1.8 mA (0.35 mW emitted power). The VCSEL is mounted on a temperature stabilized holder, which includes a 1-GHz bandwidth bias-tee in order to allow the application of short bias voltage pulses. The output beam of the VCSEL is collimated using a high numerical aperture 4.5-mm focal length lens with suitable antireflection coating. Right at the exit of the collimating lens, a zero-order half-wave plate is used to align the polarization of the emitted beam to the vertical axis. A 10% reflection beam splitter is placed after the half-wave plate in order to provide an input for the injection beam. The transmitted part of the emitted beam then passes through an optical isolator in order to shield the VCSEL from unwanted reflections. The beam is then split in two parts via a half-wave plate and a polarizing beam splitter, which directs a fraction of the output beam to a scanning Fabry Perot interferometer (Finesse 110 and 72-GHz free spectral range) and the remaing part to an optical fiber, which guides light to a 9-GHz bandwidth photodetector. The signal is acquired by a real-time oscilloscope (Wavemaster 6 GHz, 20 GS/s or DPO71254C 12.5 GHz, 100 GS/s).

The injection laser is an external grating tunable laser, which emits on a single mode of its external cavity. A 40-dB optical isolator is placed between the master laser and the VCSEL in order to obtain unidirectional coupling between both. The optical frequency of the master laser is set by discrete steps through alignment of the diffraction grating. A (polarization preserving) fiber coupled Lithium Niobate phase modulator with 10-GHz bandwidth is placed after the optical isolator in order to apply phase perturbations to the system. The phase modulator is driven by a pulse generator with 100-ps rise time. After the phase modulator, the injection beam passes through a half-wave plate and a vertical polarizer that enables control of the amount of injected power, which is of the order of a few tens of microWatts in the following.

Due to the stepwise tunability of the master laser (external mode spacing) the experiment can be performed in discrete
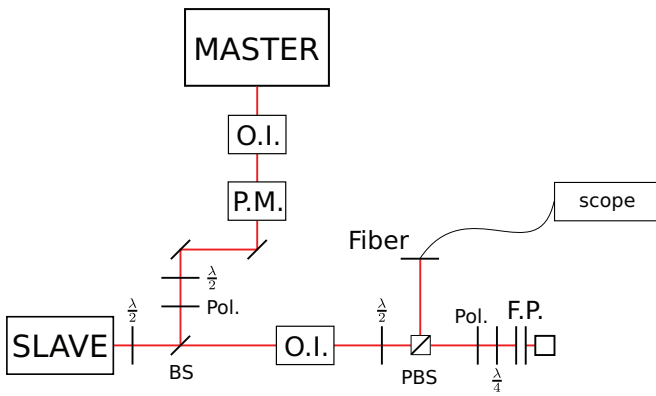
FIG. 1. (Color online) Schematic of experimental setup. O.I., optical isolator; P.M., phase modulator; $\lambda/(2|4)$, (half|quarter)-wave plate; Pol., polarizer; PBS, polarizing beam splitter; F.P., Fabry-Perot interferometer.

bias current regions of the slave laser, which correspond to VCSEL emission wavelength being close (within a few GigaHertz) to the master laser emission frequency. In each of these regions, the fine adjustment of the detuning parameter between the master and the slave laser is achieved via the VCSEL bias (frequency shift 125 GHz/mA). The dynamics of such a system depending on parameters is known to be extremely rich, but in the present case we are concerned only with the simpler case of the transition between the locked (stable fixed point) and unlocked regions (limit cycle corresponding essentially to two-frequency emission). A typical bifurcation diagram corresponding to this simple case can be obtained for very small injected power (here 30 μW) as shown in Fourier space on Fig. 2. The figure has been obtained by measuring optical spectra with the Fabry Perot interferometer for decreasing values of bias current.

The central region in Fig. 2 shows that the system is on a stable fixed point corresponding to constant emitted power at a single optical frequency: for current values between 2.04 and 1.94 mA, the slave laser is locked to the external forcing,
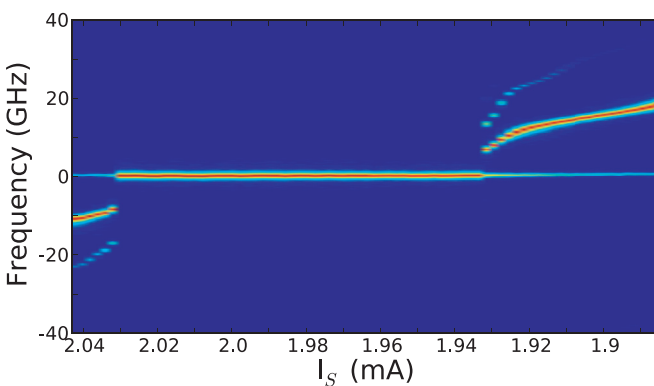
FIG. 2. (Color online) Optical spectra of the injected VCSEL as a function of the bias current. The VCSEL is locked to the forcing between 2.04 and 1.94 mA. Outside of this region, the injection level being very weak, the spectra contains mostly the master laser frequency (horizontal line), the VCSEL frequency (thick oblique lines), and a small four-wave mixing peak. The color scale is logarithmic.

whose emission frequency is taken as reference. Outside of this region, essentially two frequencies are present in the signal: the master laser's spectrum is still visible at 0 frequency, while the thick oblique line coincides with the solitary VCSEL emission frequency when the detuning is large. The slope of this thick line indicates the wavelength shift of the VCSEL with the bias current; the optical frequency increases when the bias current is reduced. The tiny harmonic observed at twice the VCSEL optical frequency is attributed to four-wave mixing and its amplitude rapidly vanishes when the VCSEL frequency shifts away from the one of the master laser. The parameter regime in which excitability essentially described by the Adler equation can be expected is when the slave laser is locked but the system is set very close to the unlocking transition. For instance, in the case of Fig. 2 the system is expected to be excitable when the bias current is set to 1.935 mA. Due to a tiny bistability region between locked and unlocked states (about 1 to 3 μA in terms of VCSEL bias current, which is very close to the resolution of the power supply, 1 μA), the following experiments are performed by first bringing the system into the locking region and then decreasing bias current down to a value very close (within 2 μA) to the unlocking transition. All measurements reported in the following have been performed in the same transition, i.e., when the optical frequency of the master laser is slightly inferior to the frequency of the standalone slave laser.

For a system to be excitable, it must possess two properties: first, there must exist some threshold in the perturbation amplitude required to trigger a noticeable response; second, this response must be independent of the perturbation provided the threshold is overcome.

We look for this threshold by applying perturbations in the phase of the injection beam. In this case, the perturbations are phase jumps of 100-ps duration. The phase modulator is driven by a square wave signal with a low repetition rate of 50 MHz in order to avoid locking phenomena [10,21]. The results are shown in Fig. 3. The efficiency is computed as the ratio between the successful perturbations (which generate the large pulses shown on the insets) and the total number of perturbations. We underline that only the upwards voltage steps, which correspond to upwards phase steps, have been observed to trigger the large responses, as is obviously expected from the position of stable and unstable fixed points in the Adler equation. Each data point corresponds to 5000 realizations. The efficiency abruptly grows from 0 to almost 1 when the phase jump is larger than approximately $60°$. The insets show the different responses, which are observed for different stimulations. When the perturbation fails (lowest inset, $52°$) almost no response is observed. On the contrary, all the responses are practically identical when the perturbation is successful (top three insets: $52°$, $60°$, $66°$). The only observed difference between the successful responses shown in the insets lies in the delay with which they actually occur with respect to the application of the perturbation.[1] This observation is fully consistent with the barrier-crossing process, which is

_____

[1]The phase perturbation is applied via the lithium niobate phase modulator placed on the path of the injection beam several meters before the VCSEL, i.e., several nanoseconds before we can observe
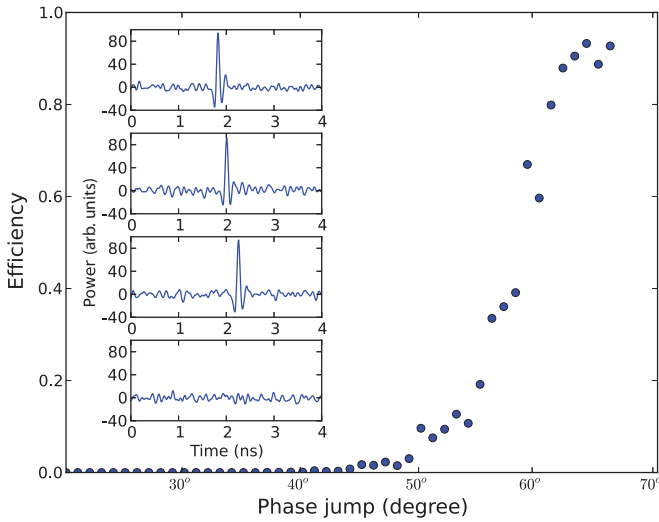
FIG. 3. (Color online) Perturbation efficiency depending on the amplitude of the phase jump. Low-amplitude phase jumps do not trigger any visible response (bottom inset, 52°), while above a certain threshold (55°) nearly all perturbations are successful. In this case, all the responses are essentially identical (top inset, 66°; second inset, 55°; third inset, 52°). The time traces were acquired with a 12.5-GHz bandwidth, 100 GS/s sampling rate real-time oscilloscope. The DC component of the signal is removed by an AC-coupled amplifier. VCSEL bias current 1.026 mA, injected power 42 μW.

expected at the onset of an excitable pulse (a phenomenon first observed in Ref. [1] and measured in a laser with saturable absorber in Ref. [7]). The fact that there is some dispersion in the time at which the excitable pulse actually takes place (within a few tens of picoseconds, not shown) is attributed to the presence of noise in the system. Another effect of noise is to slightly blur the excitability threshold, leading to an efficiency that grows smoothly instead of abruptly switching from zero to one (as studied analytically in Ref. [19]).

After having analyzed the presence of threshold, we demonstrate the independence of the response on the perturbation provided the threshold is overcome by statistically analyzing the properties of the response pulses, as shown on Fig. 4.[2] On the top panel, we show three examples of sequence of responses for increasing phase-jump amplitudes. When the phase jump is small (top panel, 34°), no visible response is observed. For large perturbations (bottom panel, 70°), almost all perturbations lead to a large response. The intermediate panel (54°) is the intermediate case showing both small and large responses. We show on the middle panel the

_____

its effects. Although the linear response is hidden in the detection noise, we have determined by averaging over 5000 realizations much below threshold that the actual phase shift takes place in the VCSEL at time 1.52 ns on the insets.

[2]Although this particular realization of the experiment was done at a bias current value for which the weak polarization of the standalone VCSEL is not strictly zero (1.935 mA), we have not observed any particular difference in the response of the system with respect to realizations in a bias range corresponding to purely single-polarization standalone emission as is the case in Figs. 3 and 5.
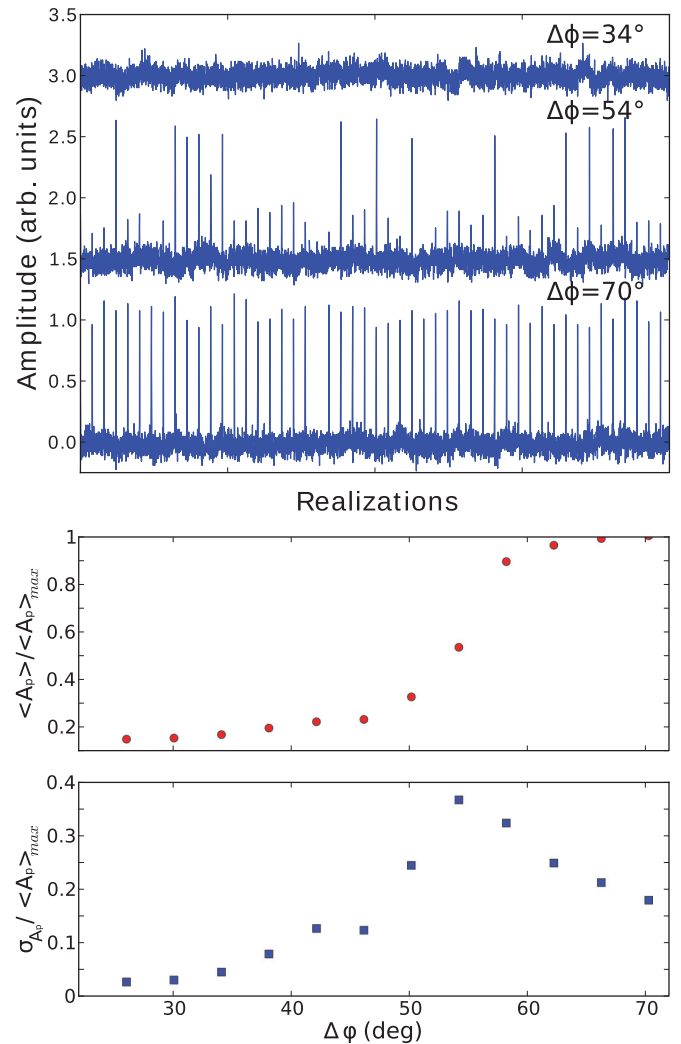
FIG. 4. (Color online) Top panel: Response to phase jumps of the injection beam depending on the phase jump height. In all cases the phase jump duration is of 100 ps. On the top trace, no response is observed. On the bottom trace, nearly all perturbations successfully trigger a response. The middle trace is the intermediate case in which either types of response can be observed. The pulses are applied at a 50-MHz repetition rate, dead time between measurements has been cut off. Bottom panels: normalized response amplitude as function of the phase jump and standard deviation of the response amplitude. VCSEL bias current 1.935 mA, injected power 30 μW.

normalized amplitude of the monitored pulses, averaged over 5000 realizations. The threshold is revealed by the strong increase of the average value of the pulse amplitude at about 55°. Correspondingly, the standard deviation of the response amplitude shown on the bottom panel clearly shows a maximum for perturbations close to 55°. This is associated to the (noise-induced) occurrence of both the linear and excitable responses when the amplitude of the perturbation is at threshold. Finally, way above threshold, for phase jumps larger than 60°, the standard deviation decreases very strongly, showing that all the responses have very similar amplitudes. We interpret the residual nonzero dispersion of the responses as a result of the limited sampling rate of the oscilloscope
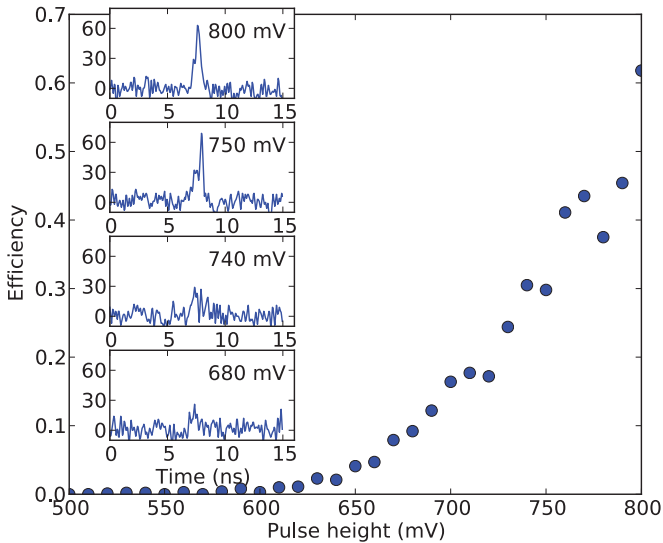
FIG. 5. (Color online) Perturbation efficiency depending on the height of the voltage pulse applied to the VCSEL. The time traces in the insets have been acquired at a 20-GS/s sampling rate with 6-GHz analog bandwidth oscilloscope. The amplitude of the excitable response is about 10% of the DC signal. The DC component has been removed. The bias current is 1.6 mA; the injected power is 93 μW.

used for this measurement (20 Gs/s), which prevents accurate detection of the pulse maximum. Even with these limitations, the strong reduction of the dispersion of the response amplitude beyond the excitability threshold is evident and confirms the unicity of the excitable trajectory.

From the previous data, the excitable character of the system has now been clearly proven since the defining properties of excitable systems have been demonstrated.

It is interesting to observe that even if a perturbation in the phase of the injection beam is expected to be the most adequate to trigger excitable pulses in such a system, other ways of perturbing the system should also lead to the observation of the typical all-or-nothing response of excitable systems. We address this issue by applying now a perturbation in the form of a voltage pulse applied to the slave device. When the parameters are chosen adequately, close to the unlocking transition for low values of bias current, the linear and excitable responses can be obtained depending on the height of the voltage pulse as illustrated in Fig. 5. As in the previous case, we show the efficiency of the perturbation depending on its amplitude. Each data point corresponds to 400 realizations of the experiment. The pulses are produced by a HP8133A pulse generator (pulse duration of 330 ps, 100-ps rise time, 730-mV amplitude) and are applied to the system via a 1-GHz bandwidth bias tee, which leads to a rather slow (order of 1 ns) current pulse. They are applied at a low repetition rate (33 MHz). Two different types of responses can be observed: if the perturbation is large enough (top two insets), the system goes through a large excursion before returning to its quiescent state and, as in the case of perturbations applied in the phase, this orbit does not depend on the perturbation except for the delay between the response and the perturbation. This delay, hardly visible on the top panel, is about 100 ps (at the edge of

the detection bandwidth) in the second panel and is responsible for the small dip separating the current pulse from the actual very short peak, which is the excitable orbit. If on the contrary the system does not reach the separatrix bringing it to the excitable orbit, the amplitude of the response is conditioned by the size of the perturbation as can be observed on the bottom two panels. In this case, the bump that is observed in the time series is the linear response to the current perturbation.

The comparison of the two methods (Figs. 3 and 5) is actually enlightening with respect to the nature of excitable systems. It is clear that the "phase jump" perturbation is much more efficient since the linear response can be hardly visible, while the excitable response is very clear. On the contrary, the voltage pulse is actually able to trigger the excitable pulses, but the system needs to be pushed away extremely far from its stable point in order to reach the separatrix, which will lead to the excitable pulse. This is a consequence of the fact that the voltage pulse does not displace the system in the optimal direction with respect to the separatrix between the linear and nonlinear responses. In fact, technical limitations in the amplitude of the voltage pulse (3.3 V) and rise time (filtered by the 1-GHz bandwidth bias tee and laser package) did not allow us to reach 100% efficiency with this method. As in the case of phase perturbations, the efficiency curve is smoothed by noise present in the system (a situation analyzed theoretically in Ref. [19]), which explains the possibility of triggering excitable pulses even when maximal efficiency is technically not attainable. Nevertheless, it is remarkable that under the application of voltage pulses or of phase jumps, the response of the system is essentially identical once some separatrix in phase space is overcome.

Besides these observations, we finally recall that excitable systems have long been envisioned as devices for information processing, not only due to the neurophysiological origin of the concept but also due precisely to their ability to respond to external stimuli with well-calibrated pulses, which do not depend on the details of the perturbation causing them. While mimicking this neuron-like response can be obtained by stacking different mechanisms as attempted, for instance, in Ref. [22], the excitable character of the system in the present experiment has allowed us to generate optical pulses shorter than 100 ps, all identical to each other, applying to phase modulator electrical pulses of several-nanoseconds duration and widely differing amplitudes. In an optics context, the control of excitable pulses via phase modulation may therefore constitute a useful scheme for the production of short and well-calibrated optical pulses. The main interest of this approach, in comparison to usual interferometric schemes, is that it requires only a short rise time (instead of a short pulse) and does not critically depend on the amplitude or duration of the input pulses. More importantly, from a very general point of view, the ability to trigger the excitable response of this system via optical or electrical perturbations is key to any information processing approach involving one or many coupled optical excitable units.

[1] A. L. Hodgkin, A. F. Huxley, and B. Katz, J. Physiol. **116**, 424 (1952).

[2] A. Hodgkin and A. Huxley, J. Physiol. **117**, 500 (1952).

[3] R. A. FitzHugh, Biophys. J. **1**, 445 (1961).

[4] J. Keener and J. Sneyd, *Mathematical Physiology: I: Cellular Physiology*, Vol. 1 (Springer, Berlin, 2008).

[5] I. R. Epstein and J. A. Pojman, *An Introduction to Nonlinear Chemical Dynamics: Oscillations, Waves, Patterns, and Chaos* (Oxford University Press, New York, 1998).

[6] F. Plaza, M. G. Velarde, F. T. Arecchi, S. Boccaletti, M. Ciofini, and R. Meucci, Europhys. Lett. **38**, 85 (1997).

[7] M. A. Larotonda, A. Hnilo, J. M. Mendez, and A. M. Yacomotti, Phys. Rev. A **65**, 033812 (2002).

[8] S. Barbay, R. Kuszelewicz, and A. M. Yacomotti, Opt. Lett. **36**, 4476 (2011).

[9] M. Giudici, C. Green, G. Giacomelli, U. Nespolo, and J. R. Tredicce, Phys. Rev. E **55**, 6414 (1997).

[10] S. Barland, O. Piro, M. Giudici, J. R. Tredicce, and S. Balle, Phys. Rev. E **68**, 036209 (2003).

[11] T. V. Vaerenbergh, M. Fiers, P. Mechet, T. Spuesens, R. Kumar, G. Morthier, B. Schrauwen, J. Dambre, and P. Bienstman, Opt. Express **20**, 20292 (2012).

[12] A. M. Yacomotti, P. Monnier, F. Raineri, B. B. Bakir, C. Seassal, R. Raj, and J. A. Levenson, Phys. Rev. Lett. **97**, 143904 (2006).

[13] M. Brunstein, A. M. Yacomotti, I. Sagnes, F. Raineri, L. Bigot, and A. Levenson, Phys. Rev. A **85**, 031803 (2012).

[14] P. Coullet, D. Daboussy, and J. R. Tredicce, Phys. Rev. E **58**, 5347 (1998).

[15] R. Adler, Proc. IRE **34**, 351 (1946).

[16] D. Goulding, S. P. Hegarty, O. Rasskazov, S. Melnik, M. Hartnett, G. Greene, J. G. McInerney, D. Rachinskii, and G. Huyet, Phys. Rev. Lett. **98**, 153903 (2007).

[17] B. Kelleher *et al.*, Opt. Lett. **34**, 440 (2009).

[18] B. Kelleher, C. Bonatto, G. Huyet, and S. P. Hegarty, Phys. Rev. E **83**, 026207 (2011).

[19] F. Pedaci, Z. Huang, M. van Oene, S. Barland, and N. H. Dekker, Nat. Phys. **7**, 259 (2010).

[20] L. Kuhnert, K. Agladze, and V. Krinsky, Nature (London) **337**, 244 (1989).

[21] M. Feingold, D. L. Gonzalez, O. Piro, and H. Viturro, Phys. Rev. A **37**, 4060 (1988).

[22] K. Kravtsov, M. P. Fok, D. Rosenbluth, and P. R. Prucnal, Opt. Express **19**, 2133 (2011).